Microsyst Technol (2016) 22:2125–2131
DOI 10.1007/s00542-015-2641-1

CrossMark

TECHNICAL PAPER

Thermomechanical behavior of bulk NiTi shape-memory-alloy microactuators based on bimorph actuation

Alaa AbuZaiter[1] · Marwan Nafea[1] · Ahmad Athif Mohd Faudzi[1] · Suhail Kazi[2] · Mohamed Sultan Mohamed Ali[1,3]

Received: 22 March 2015 / Accepted: 23 July 2015 / Published online: 7 August 2015
© Springer-Verlag Berlin Heidelberg 2015

Abstract Shape-memory-alloy (SMA) has attracted considerable attention in recent years as a smart and efficient material, due to its unique properties. SMA microactuators became one of the potential solutions for unresolved issues in microelectromechanical systems (MEMS). This paper presents a thermomechanical behavior analysis of bimorph SMA structure and studies the effect of varying the SMA layer thickness, the type of stress layer and its thickness, and the processing temperature on the displacement of the microactuator. Furthermore, the analyzed results were verified by experimental work, where the fabrication of the SMA microactuators followed the standards of the MEMS fabrication process. SiO_2, Si_3N_4 and Poly-Si were used as stress layers. The fabrication results showed that the bimorph SMA structure achieved maximum displacement when SiO_2 was used. The SMA structure with dimensions of 10 mm (length) × 2 mm (width) × 80 µm (thickness), had maximum displacement of 804 µm when 4.1 µm of SiO_2 layer was deposited at a temperature of 400 °C.

1 Introduction

Microelectromechanical systems (MEMS) utilize various types of microactuators that allow microenvironments to be accessed and controlled. Their rapid advancements offer many benefits to applications in microscale, especially in the biomedical field (Erismis et al. 2010; Nisar et al. 2008), microrobotics (Donald et al. 2006) and telecommunication (Rangra et al. 2005). Microactuators can be classified based on their actuating principles into electrostatic, electromagnetic, piezoelectric, thermal and shape-memory-alloy (SMA) actuators (Bell et al. 2005). These actuators have their own properties and advantages that allow them to be used in various applications, based on the specific requirements of those applications.

Electrostatic microactuators have been applied in many applications such as hard disc drives and aeronautical fields (Fan et al. 1999; Rashedin et al. 2006). These actuators provide fast response, small energy loss and reversible motion, while they often suffer from a limited displacement range, short lifetime and high voltage requirements for their operation (Donald et al. 2006; Nisar et al. 2008). Electromagnetic microactuators have been utilized in several devices, such as micropumps and optical switches (Chang et al. 2007; Su and Chen 2007). However, this type requires complicated control systems, due to its magnetic nature (Braun et al. 2009). Piezoelectric microactuators are applied extensively in printers and digital cameras (Uchino 2008), due to their fast response, high accuracy and large stress tolerance (Nafea et al. 2014). Despite their advantages, piezoelectric actuators require high actuation voltages and involve a complicated fabrication process, which make them uncomplimentary (Liu et al. 2014). Thermal microactuators have limited applications compared to other types of actuators, for their slow response, high power consumption and the high temperature required for actuation (Iamoni and Somà 2014). One of the most popular types of thermal microactuators is the bimorph actuator, which actuates using the difference in the coefficient of thermal expansion (CTE) of two different materials.

✉ Mohamed Sultan Mohamed Ali
sultan_ali@fke.utm.my

1 Faculty of Electrical Engineering, Universiti Teknologi Malaysia, 81310 Skudai, Johor, Malaysia

2 Faculty of Mechanical Engineering, Universiti Teknologi Malaysia, 81310 Skudai, Johor, Malaysia

3 Flextronics, Pelabuhan Tanjung Pelepas (PTP), 81560 Gelang Patah, Johor, Malaysia

Utilizing SMA material is an emerging technique that overcomes some of the major drawbacks in thermal microactuators. SMA microactuators offer various advantages, such as high work density, large actuation force, simple mechanical structures, resistance to corrosion, low cost, biocompatibility and large displacement range (Stirling et al. 2011). These factors give SMA microactuators unique advantages over other actuation techniques. SMA actuators have been applied in several areas, such as microrobotics (Donald et al. 2006), micropumps (Xuesong et al. 2009), medical tools and biomedical applications (Fu et al. 2004). The actuation principle of SMA actuators can be classified into two actuating methods. The first method is called "two-way SMA actuation", which allows an SMA actuator to remember its shape in the austenite phase (the high temperature phase) and martensite phase (the low temperature phase) (Mehrabi et al. 2013). This method allows actuation in two directions. However, the SMA tends to lose its original shape after several actuations and does not return to the desired position. This reduces the accuracy of SMA microactuators, which makes this method unfavorable. The second actuation method is called "one-way actuation", which allows the SMA to actuate to its original shape when the temperature reaches the austenite phase. However, this method requires the application of an external force, such as a spring, to actuate the SMA back to its cold-state shape (Nespoli et al. 2010; Pemble and Towe 1999). This constrains its use in microdevices, in which the handling and space are crucial factors. A promising method has been reported to cause a reversed force by depositing a stress layer onto the SMA material. As a result of the CTE mismatch between the SMA and stress layers, the structure will bend and provide displacement in cold (martensite) state (Mohamed Ali and Takahata 2010). This method is similar to the bimorph-type actuator, except that the SMA actuators only require austenitic phase temperature for maximum displacement, in contrast to conventional bimorph actuators, which need a very high temperature for maximum actuation (Braun et al. 2009). The transformation phase temperature of the SMA totally depends on the material composition. A MEMS-based SMA microactuator mainly includes nickel and titanium alloy (nitinol). The composition level of these metals will essentially determine the transformation temperature. Thus, the composition can be intentionally changed in order to achieve a specific transformation temperature. This offers great flexibility to apply SMA microactuators for various applications depending on the suitable temperature range (from −50 to 110 °C) (Braun et al. 2009).

Several actuation mechanisms of SMA microactuators were described, including external joule heating using heaters to heat up the SMA (Mohamed Ali et al. 2014) and internal heating by passing current through the SMA parts (Mineta et al. 2011; Pieczyska et al. 2014). These are among the most widely used methods for actuating SMA microactuators (Jani et al. 2014). The concept of manufacturing bimorph bulk SMA microactuators was introduced to reduce the power consumption of the microactuator and to eliminate the potential mechanical weakening of the SMA material.

This paper reports on the thermomechanical behavior of SMA bimorph microactuators and analyses the displacement level of the structure when four parameters (the SMA sheet thickness, the type of the deposited material, the thicknesses of the deposited layer and the deposition temperature) are varied. The working principle of the SMA bimorph microactuators and the effect of the four parameters mentioned above on the displacement are highlighted, and the simulation results of the thermomechanical behavior of the SMA bimorph microactuators are presented. Moreover, the effects of the thickness of the SMA layer, the thickness of the stress layers and the deposition temperature on the displacement are studied. The results are accomplished using the finite element analysis (FEA) method via COMSOL Multiphysics. The fabrication process and results of SMA microactuators that have different thickness values of their SMA and stress layers are also described. The outcomes of using three materials (SiO_2, Poly-Si and Si_3N_4) as stress layers are studied and experimentally verified.

2 Working principle and design

This section discusses the working principle of the SMA bimorph microactuator under study. Bimorph actuation depends on the difference in CTE between two materials, i.e. SMA material and the stress layers deposited on top of SMA (Poly-Si, SiO_2 and Si_3N_4 in this case). When the stress layer is deposited onto the surface of the SMA sheet at a high temperature (usually in hundreds of degrees Celsius), a stress will be induced when the SMA is cooled down to room temperature due to the mismatch in CTE between these two materials (SMA and the stress layer). This stress will cause the curvature, r, of the structure to extend depending on the amount of stress applied in cold state (Fig. 1). For the returning motion, the actuator only needs to be heated to SMA's austenitic phase temperature (hot state) instead of the deposition temperature, which is a lot higher.

When one end of the SMA cantilever is fixed, a specific displacement can be measured at the other end in cold state. The level of displacement of the SMA actuator can be controlled by varying the thicknesses of the materials, including the SMA sheet and the stress layer, and by varying the temperature used during deposition of the stress layer. The displacement forms the arc whose radius of curvature, r, can be expressed as:

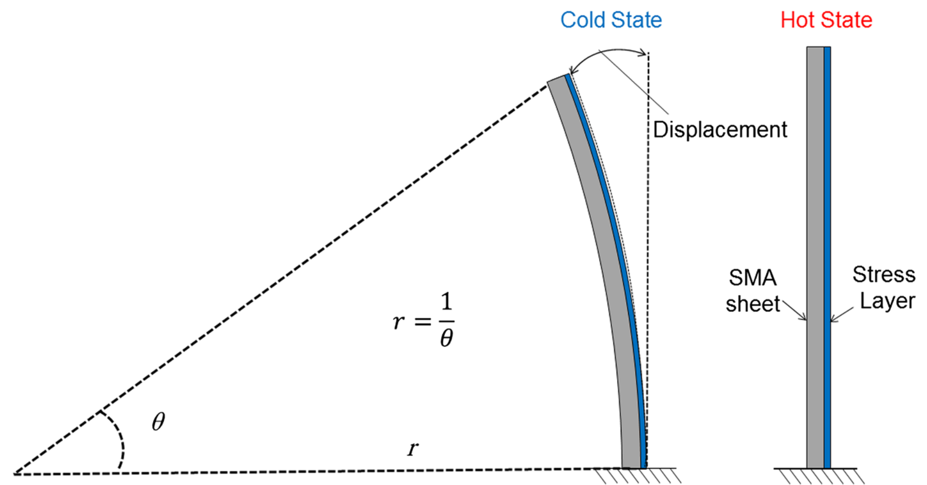

Fig. 1 The design and working principle of a bimorph SMA microactuator during hot and cold states

Table 1 Microactuator design parameters

Properties	Values
Thickness of SMA (μm)	50, 60, … 200
Thickness of stress layer (μm)	1, 2, … 6
Deposition temperature (°C)	200, 250, … 500

$$r = \frac{\left(w_1E_1t_1^2\right)^2 + \left(w_2E_2t_2^2\right)^2 + 2w_1w_2E_1E_2t_1t_2\left(2t_1^2 + 3t_1t_2 + 2t_2^2\right)}{6w_1w_2E_1E_2t_1t_2(t_1 + t_2)(\alpha_1 - \alpha_2)\Delta T} \quad (1)$$

where E is Young's modulus of the materials, w is the width of the beam, t is the thickness of the layer, α is CTE, ΔT is the temperature difference between the initial flat condition and the deformed state, and subscripts 1 and 2 represent the SMA and the stress layer, respectively.

The displacement characterization in the cold state is performed using FEA by COMSOL Multiphysics software. The SMA material used is nitinol (45 % Ti and 55 % Ni), with a fixed length and width of 10 and 3 mm, respectively. The thickness of the SMA sheet and the stress layers (SiO2, Poly-Si and Si3N4), and the depositing temperature are varied according to Table 1.

For the purpose of the analysis, the SMA sheets was fixed at one end so that the displacement can be measured at the free end as shown in Fig. 1. All the displacement measurements were taken at room temperature (21 °C). The thermomechanical properties of SMA and stress layers are defined as in Tables 2 and 3, respectively (AbuZaiter and Mohamed Ali 2014).

Table 2 Thermomechanical properties of nitinol (Davis 2005)

Properties	Values
Coefficient of thermal expansion (1/K)	6.6×10^{-6} (martensite phase) 11×10^{-6} (austenite phase)
Density (kg/m^3)	6450
Young's modulus (Pa)	20.6×10^9–70.33×10^9
Poission's ratio	0.3

Table 3 Thermomechanical properties of stress layer material (Fu et al. 2005; Johnson and Rowcliffe 1985; Tada et al. 2000)

Properties	SiO_2	Poly-Si	Si_3N_4
Coefficient of thermal expansion (1/K)	0.5×10^{-6}	2.6×10^{-6}	2.3×10^{-6}
Density (kg/m^3)	2200	2320	3100
Young's modulus (Pa)	70×10^9	160×10^9	250×10^9
Poission's ratio	0.17	0.22	0.23

3 Simulation results and discussions

This section presents the simulation results of the thermomechanical behavior of SMA bimorph microactuator. The simulations were performed to determine the displacement of the bimorph SMA microactuator by varying the thickness of the SMA and the stress layers, and the deposition temperature. The analyses of the characteristics of the SMA microactuator are presented in the following sections. The performance was evaluated through the amount of displacement it undergoes when the thickness of the SMA and the stress layers, and the deposition temperature, were varied (Davis 2005; Johnson and Rowcliffe 1985; Tada et al. 2000). As an example of FEA, Fig. 2 demonstrates the maximum displacement (1057 μm) of the SMA microactuator that consists of a 5 μm layer of SiO_2 deposited on a 70 μm layer of SMA sheet at 400 °C.

The following subsections independently present, the effect of varying the thickness of the SMA and the stress

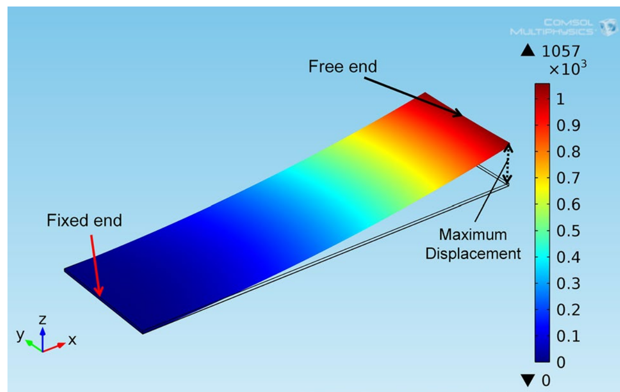

Fig. 2 FEA displacement result when the deposition temperature is 400 °C, the SMA sheets with dimensions (3 mm × 10 mm × 70 μm) and stress layer (SiO_2) thicknesses 5 μm

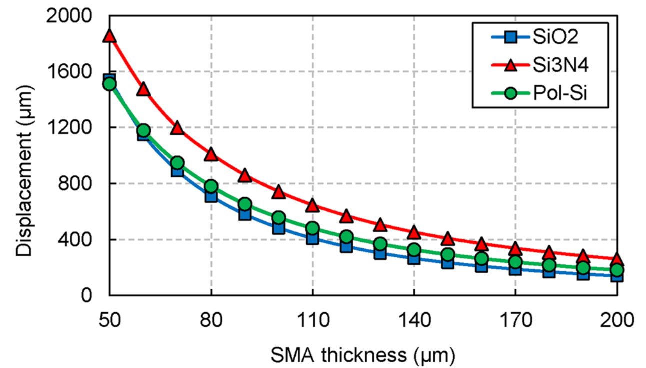

Fig. 3 Displacement of SMA by changing the thickness of the SMA sheet using different stress layers

layers, and the deposition temperature, on the displacement of the microactuator.

3.1 The effect of the SMA thickness on bending

The mismatch of CTE between the SMA and the stress layer material has a significant effect on the displacement of the SMA microactuator. In addition, the amount of displacement also depends on the thickness of the SMA material. To optimize the SMA thickness, a study was performed by keeping the deposited material (SiO_2, Poly-Si and Si_3N_4) thickness and the temperature constant at 4 μm and 400 °C, respectively. The results in Fig. 3 show the change in the displacement when the thickness of the SMA structure was varied.

From the graph, it can be seen that increasing the thickness has a negative effect on the displacement. The results show that when the thickness of the SMA was 50 μm, the displacements were 1859, 1541 and 1512 μm for the Si_3N_4, SiO_2 and Poly-Si stress layers, respectively. On the other hand, when the thickness was increased to 200 μm, the displacements decreased to 263, 141 and 184 μm for Si_3N_4, SiO_2 and Poly-Si, respectively. This variation in the displacement is caused by the change in the stress generated between the SMA layer and the stress layer in each case. For each material, the reduction in displacement occurs due to the increment in the amount of stress that the SMA layer can exert when its thickness is increased. A relatively thin SMA layer has a very low yield strength, which allows the microactuator to achieve higher displacement in cold state (Braun et al. 2009). Further observations in Fig. 3 show that the amount of displacement dropped dramatically when the thickness of the SMA layer was reduced to lower values another observation was, the difference in the amount of displacement started to slowly converge at higher thickness values of the SMA layer. For instance, increasing the thickness of the SMA layer from 50 to 60 μm led to a reduction in the displacement by 25.38 %, while it was only 8.72 % when the SMA layer thickness increased from 190 to 200 μm. This was caused by the change in the ratio of the thickness of the SMA layer (50–200 μm) to the thickness of the stress layer (4 μm), thereby increasing the radius of the curvature in Eq. (1).

3.2 The effect of the stress layer thickness on bending

Some applications require high actuation force, which consequently require higher thickness values of the SMA layer. However, a high SMA layer thickness limits the displacement of the microactuator. Thus, varying the SMA layer thickness to achieve a specific displacement is not always a possible option.

One of the simpler ways to adjust the displacement level is by varying the thickness of the stress layer. Figure 4 shows the displacement of the SMA when the thickness of the stress layers were varied between 1 and 6 μm, while keeping the deposition temperature and the thickness of the SMA constant at 400 °C and 100 μm, respectively.

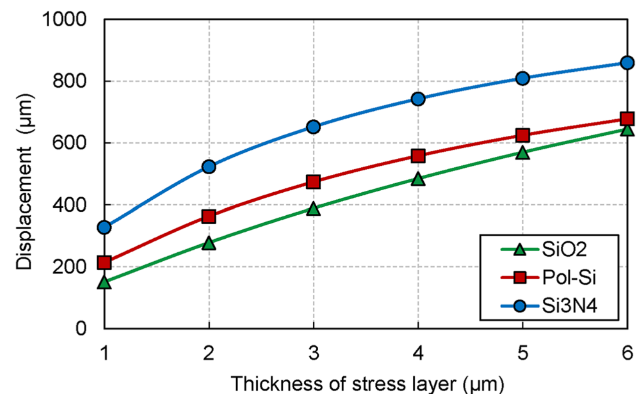

Fig. 4 Displacements of SMA vs. thickness of stress layer

The thickness of the stress layer has a positive effect on the displacement in contrast to the SMA thickness (as described in the previous section). The results indicate that when the stress layers thicknesses were increased from 1 to 6 µm, the displacements showed an increasing trend in all the stress layer types used. For instance, an increment of 326.23, 216.41 and 162.17 % was observed when SiO_2, Poly-Si and Si_3N_4 were used, respectively. The difference between the three ratios can be explained as the result of the thermomechanical properties of the materials of the stress layer (SiO_2, Poly-Si, and Si_3N_4), as stated earlier in Table 1. It is indicated that Si_3N_4 has the highest displacement values for all the thickness ranges, while SiO_2 shows the lowest displacement range. However, it is not practical to deposit a very thick Si_3N_4 layer, as the deposition process takes a very long time and it may lead to cracking the stress layer (Fu et al. 2005). Moreover, Poly-Si shows poor adhesion to SMA (Krulevitch et al. 1996). Thus, SiO_2 was considered as the most suitable material to achieve good displacement with reliable results.

3.3 Deposition temperature effect on displacement

The deposition temperature of the stress layer contributes to the level of curvature and the displacement of the SMA bimorph microactuator as stated earlier in Eq. (1). This section focuses on analyzing the effect of the temperature using SiO_2 as a stress layer, due to its advantages over the other materials. The most practical method for achieving an optimum displacement is by simply changing the temperature of the deposition chamber. As illustrated in Fig. 5, when depositing SiO_2 at different temperatures while keeping the thickness of SMA and SiO_2 layers constant, the displacement amount varied. For example, keeping the thickness of the SMA at 70 µm and SiO_2 at 5 µm, while changing the temperature from 200 to 500 °C, caused the displacement of the SMA to increase by 814.13 µm.

The deflection of each SMA microactuator was a result of the strain mismatch between the SMA and the SiO_2 layers, due to temperature rise. When the temperature increased, the SMA layer will have both contracting and expanding properties due to shape memory effect and thermal effect, respectively. On the other hand, SiO_2 has thermal expansion only, which causes a mismatch in CTE between the two layers. As the temperature raised, this mismatch increased and caused the SMA microactuator to deflect more.

4 Experimental characterization

This section presents the fabrication process and results of three SMA bimorph microactuators with different thickness values of SMA and stress layers.

4.1 Fabrication process

The fabrication process is divided into four stages as shown in Fig. 6. An SMA sheet (SAES Memory, Germany) with a transformation temperature of 65 °C and 100 µm thickness was used. First, the SMA sheet was covered with a masking layer, except for the surface that needed to be etched. Then, the SMA sheet was etched in an HNA solution [nitric acid (HNO_3) 30 % + hydrofluoric acid (HF) 20 % + DI water (H_2O) 50 %] to reduce the thickness of the SMA sheet to 80 µm. The etching rate observed was 2 µm/min. In the third step, the SMA sheet was cut to the desired dimensions by using a micro-electrical-discharge machining (µEDM, EM203, SmalTec International, IL, USA), where the length and the width of the microactuators were 10 and 2 mm, respectively. Lastly, the stress layer (SiO_2) was deposited

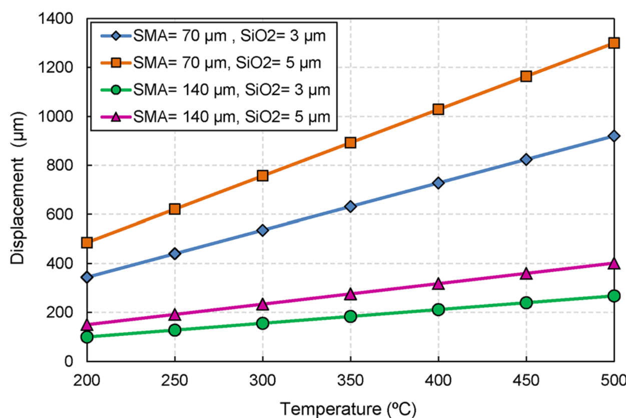

Fig. 5 Displacement of different SMA microactuators vs. deposition temperature

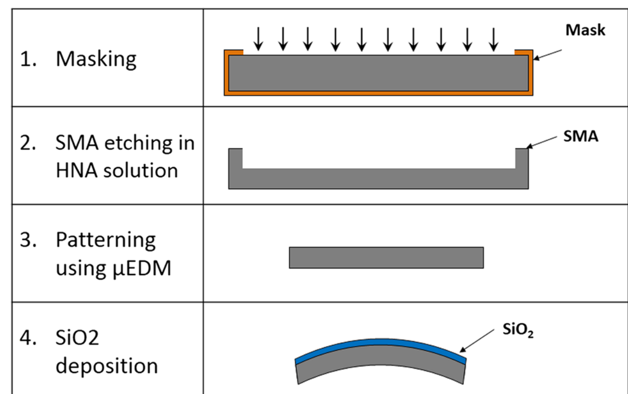

Fig. 6 Fabrication process of the microactuator

on top of the SMA sheet at 350 °C using plasma enhanced chemical vapor deposition (PECVD) with a deposition rate of 1 nm/s. Thus, the deposition time of actuators 1 and 2 was 3500, and 2400 s for actuator 3.

4.2 Fabrication results

The actuators were fabricated with different thicknesses of SMA and stress layers. As shown in Table 4, the first and the second SMA actuators have a 4.1 µm SiO_2 stress layer thickness, and a 100 and 80 µm SMA layers thickness, respectively). The third SMA actuator has the same thickness as the SMA layer with the second actuator (80 µm), while it has a different stress layer thickness (3.4 µm). The results of fabrication are as shown in Fig. 7.

The results from the fabricated device were similar to the simulation results. The displacement decreased when the thickness of the SMA layer increased, while it also decreased by increasing the thickness of the stress layer (SiO_2). The effect of the thickness of the SMA and the stress layers on the displacement is illustrated in Fig. 8. It can be seen clearly that decreasing the thickness of the SMA layer has a positive effect on the displacement, while decreasing the thickness of the stress layer has a negative effect on the displacement. These results verify the simulation results presented in Sect. 3. Furthermore, these results show that achieving the desired displacement of the SMA microactuator can be accomplished by varying the thickness of the SMA and the stress layers.

Table 4 The layer thickness of the fabricated microactuators

SMA actuator	SMA thickness (µm)	SiO_2 thickness (µm)
1	100	4.1
2	80	4.1
3	80	3.4

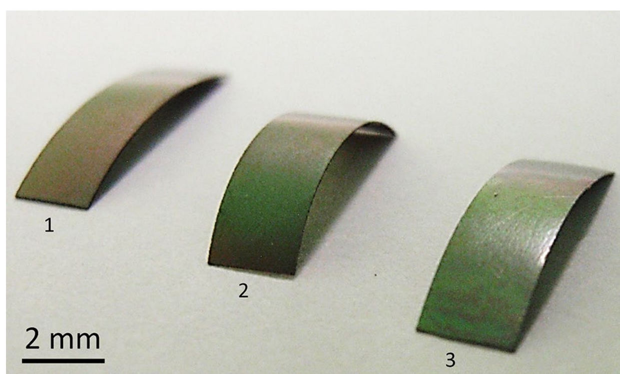

Fig. 7 Three fabricated SMA actuators

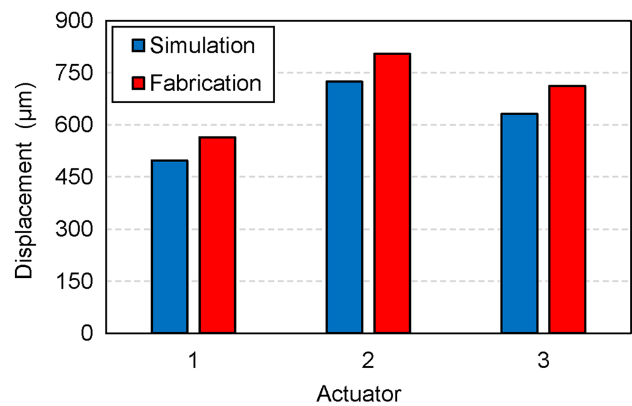

Fig. 8 Comparison of simulation and fabrication results for displacement of the SMA actuators

5 Conclusion and future work

This paper presented displacement analyses of an SMA bimorph microactuator when stress layers were deposited onto its surface using a finite element model. The analyses were performed in various conditions by varying the thickness of the SMA and the stress layers, varying the deposition temperature and also by applying different stress layers. SMA bimorph microactuators have been fabricated using a MEMS fabrication process to verify the simulation results. Both the simulation and experimental results showed that the displacement of the SMA microactuator was increased when the thickness of the SMA sheet was decreased. The displacement was also affected by the type of the stress layer material and the thickness applied (SiO_2, Poly-Si and Si_3N_4). Although Poly-Si and Si_3N_4 proved to have larger displacement, SiO_2 is recommended in practical applications, as it has good adhesion to SMA and deposition of a thick layer is possible. Higher deposition temperature was seen to provide larger displacement. However, this will induce excessive stress and might cause cracking in the stress layer. In this work, a maximum displacement of 804 µm was achieved using a 4.1 µm-thick SiO_2 stress layer at 400 °C onto an 80 µm-thick SMA structure with a length of 10 mm. Future work will include the development of a new structure of a micromanipulator by integrating multiple SMA microactuators. The design will aim to develop a micromanipulator with high degree of freedom, small size and a simple actuation mechanism. Furthermore, the biocompatibility of the SMA bimorph microactuator will be considered to extend the range of applications of the micromanipulator to medical applications, such as microsurgery tools.

Acknowledgments This work was supported by a Research University Grant (10H40) from Universiti Teknologi Malaysia (UTM),

FRGS (4F386) and PRGS (4L625) Funds from Ministry of Higher Education Malaysia (MOHE), and the E-Science Fund (4S088) from the Ministry of Science Technology and Innovation Malaysia (MOSTI). Marwan Nafea's doctorate study was supported by the Malaysian Technical Cooperation Programme (MTCP).

References

AbuZaiter A, Mohamed Ali MS (2014) Analysis of thermomechanical behavior of shape-memory-alloy bimorph microactuator. In: 5th International Conference on Intelligent Systems Modelling Simulation (ISMS), Langkawi, Malaysia, 2014. IEEE, pp 390–393, 27–29 Jan 2014

Bell D, Lu T, Fleck N, Spearing S (2005) MEMS actuators and sensors: observations on their performance and selection for purpose. J Micromech Microeng 15:S153–S164

Braun S, Sandstrom N, Stemme G, van der Wijngaart W (2009) Wafer-scale manufacturing of bulk shape-memory-alloy microactuators based on adhesive bonding of titanium–nickel sheets to structured silicon wafers. J Microelectromech Syst 18:1309–1317

Chang H-T, Lee C-Y, Wen C-Y (2007) Design and modeling of electromagnetic actuator in mems-based valveless impedance pump. Microsyst Technol 13:1615–1622

Davis BA (2005) Investigation of the thermomechanical response of shape memory alloy hybrid composite beams. North Carolina State University, Raleigh

Donald BR, Levey CG, McGray CD, Paprotny I, Rus D (2006) An untethered, electrostatic, globally controllable MEMS microrobot. J Microelectromech Syst 15:1–15

Erismis MA, Neves HP, De Moor P, Puers R, Van Hoof C (2010) A water-tight packaging of MEMS electrostatic actuators for biomedical applications. Microsyst Technol 16:2109–2113

Fan L-S et al (1999) Electrostatic microactuator and design considerations for HDD applications. IEEE Trans Magn 35:1000–1005

Fu Y, Du H, Huang W, Zhang S, Hu M (2004) TiNi-based thin films in MEMS applications: a review. Sens Actuators A 112:395–408

Fu Y, Du H, Zhang S, Ong SE (2005) Effects of silicon nitride interlayer on phase transformation and adhesion of TiNi films. Thin Solid Films 476:352–357

Iamoni S, Somà A (2014) Design of an electro-thermally actuated cell microgripper. Microsyst Technol 20:869–877

Jani JM, Leary M, Subic A, Gibson MA (2014) A review of shape memory alloy research, applications and opportunities. Mater Des 56:1078–1113

Johnson SM, Rowcliffe DJ (1985) Mechanical properties of joined silicon nitride. J Am Ceram Soc 68:468–472

Krulevitch P, Lee AP, Ramsey PB, Trevino JC, Hamilton J, Northrup MA (1996) Thin film shape memory alloy microactuators. J Microelectromech Syst 5:270–282

Liu G, Yang Z, Liu J, Li X, Wang H, Zhao T, Yang X (2014) A low cost, high performance insulin delivery system based on PZT actuation. Microsyst Technol 20:2287–2294

Mehrabi K, Bruncko M, Kneissl A (2013) Investigation of bending trainings, transformation temperatures, and stability of two-way shape memory effect in NiTi-based ribbons. J Mater Eng Perform 22:1443–1452

Mineta T, Kudoh S, Makino E, Kawashima T, Shibata T (2011) Accurate and simple assembly process of shape memory alloy tubular micro manipulator with a bias mechanism. Microelectron Eng 88:2683–2686

Mohamed Ali MS, Takahata K (2010) Frequency-controlled wireless shape-memory-alloy microactuators integrated using an electroplating bonding process. Sens Actuators A 163:363–372

Mohamed Ali MS, AbuZaiter A, Schlosser C, Bycraft B, Takahata K (2014) Wireless displacement sensing of micromachined spiral-coil actuator using resonant frequency tracking. Sensors 14:12399–12409

Nafea M, Mohamed Z, Abdullahi AM, Ahmad MA, Husain AR (2014) Dynamic hysteresis based modeling of piezoelectric actuators. J Teknol 67:9–13

Nespoli A, Besseghini S, Pittaccio S, Villa E, Viscuso S (2010) The high potential of shape memory alloys in developing miniature mechanical devices: a review on shape memory alloy mini-actuators. Sens Actuators A 158:149–160

Nisar A, Afzulpurkar N, Mahaisavariya B, Tuantranont A (2008) MEMS-based micropumps in drug delivery and biomedical applications. Sens Actuators B 130:917–942

Pemble CM, Towe BC (1999) A miniature shape memory alloy pinch valve. Sens Actuators A 77:145–148

Pieczyska E, Staszczak M, Dunić V, Slavković R, Tobushi H, Takeda K (2014) Development of stress-induced martensitic transformation in TiNi shape memory alloy. J Mater Eng Perform 23:2505–2514

Rangra K et al (2005) Symmetric toggle switch—a new type of rf MEMS switch for telecommunication applications: design and fabrication. Sens Actuators A 123:505–514

Rashedin R, Meydan T, Borza F (2006) Electromagnetic microactuator array for loudspeaker application. Sens Actuators A 129:118–120

Stirling L, Yu C-H, Miller J, Hawkes E, Wood R, Goldfield E, Nagpal R (2011) Applicability of shape memory alloy wire for an active, soft orthotic. J Mater Eng Perform 20:658–662

Su Y, Chen W (2007) Investigation on electromagnetic microactuator and its application in micro-electro-mechanical system (MEMS). In: International Conference on Mechatronics and Automation (ICMA), Harbin, China, 2007. IEEE, pp 3250–3254, 5–8 Aug 2007

Tada H et al (2000) Thermal expansion coefficient of polycrystalline silicon and silicon dioxide thin films at high temperatures. J Appl Phys 87:4189–4193

Uchino K (2008) Piezoelectric actuators 2006. J Electroceram 20:301–311

Xuesong S, Yanling H, Shuxiang G, Xiufen Y, Xiaonan Y (2009) The development of a new type of compound peristaltic micropump. In: IEEE International Conference on Robotics Biomimetic (ROBIO), Bangkok, Thailand, 2009, pp 698–702, 22–25 Feb 2009